NANO LETTERS

Letter

pubs.acs.org/NanoLett

Electrical Probing and Tuning of Molecular Physisorption on Graphene

Girish S. Kulkarni,[†] Karthik Reddy,[†,‡] Wenzhe Zang,[†] Kyunghoon Lee,[†] Xudong Fan,[*,‡] and Zhaohui Zhong[*,†]

[†]Department of Electrical Engineering and Computer Science, University of Michigan, 1301 Beal Avenue, Ann Arbor, Michigan 48109, United States

[‡]Department of Biomedical Engineering, University of Michigan, 1101 Beal Avenue, Ann Arbor, Michigan 48109, United States

Supporting Information

ABSTRACT: The ability to tune the molecular interaction electronically can have profound impact on wide-ranging scientific frontiers in catalysis, chemical and biological sensor development, and the understanding of key biological processes. Despite that electrochemistry is routinely used to probe redox reactions involving loss or gain of electrons, electrical probing and tuning of the weaker noncovalent interactions, such as molecular physisorption, have been challenging, primarily due to the inability to change the work function of conventional metal electrodes. To this end, we report electrical probing and tuning of the noncovalent physisorption of polar molecules on graphene surface by using graphene nanoelectronic heterodyne sensors. Temperature-dependent molecular desorptions for six different polar molecules were measured in real-time to study the desorption kinetics and extract the binding affinities. More importantly, we demonstrate electrical tuning of molecule−graphene binding kinetics through electrostatic gating of graphene; the molecular desorption can be slowed down nearly three times within a gate voltage range of 15 V. Our results provide insight into small molecule−nanomaterial interaction dynamics and signify the ability to electrically tailor interactions, which can lead to rational designs of complex chemical processes for catalysis and drug discovery.

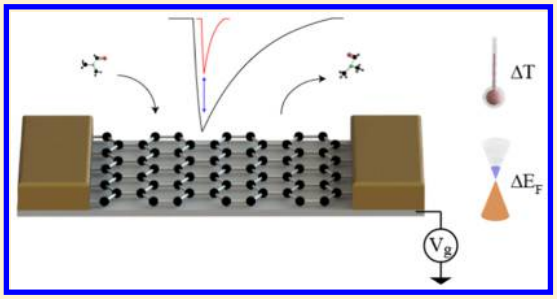

KEYWORDS: *Noncovalent interaction, physisorption, electrical tuning, graphene, binding energy, heterodyne sensor*

The behavior of molecules near a surface is dictated by the interplay of attractive and repulsive forces between the two, and these interactions can be classified as either chemical (covalent/ionic) or physical (noncovalent). Covalent interactions involve sharing of electrons between the two systems and are strong with interaction energies between 1 and 10 eV.[1] On the other hand, electrostatic noncovalent interactions are much more subtle and have interaction energy of only a few 100 meVs[1] (Figure 1a). Even though noncovalent interactions are weak, they are precise in nature, work in a time dependent manner, and are the bedrock of important chemical and biological processes.[2,3] Understanding and controlling these noncovalent interactions can usher new scientific and technological breakthroughs in the area of catalysis,[4,5] drug-discovery,[6,7] proteomics,[8] combinatorial chemistry,[9] supramolecular chemistry,[10] and environmental remediation.[11] While redox reactions and covalent interactions can be studied by electrochemistry, electrical probing and tuning of noncovalent interactions have not been possible due to the inability to change the work functions (or Fermi levels) of conventional metal electrodes.

Miniature analytical systems based on nanomaterials like carbon nanotubes, nanowires, graphene, and transition metal dichalcogenides offer a great platform to study the physicochemical nature of such interactions due to their large surface-to-volume ratios, exceptional electronic properties, chemical stability in different environments, and compatibility with modern processing technologies.[12−15] Most importantly, the reduced density-of-states in low dimensional nanomaterials provides the capability of electrostatic tuning of the charge densities and hence their Fermi levels. As shown in Figure 1a, the range of gate tunability in a typical nanomaterial device is on the order of ±0.5 eV, which conveniently covers the energy range for weak noncovalent interactions. Furthermore, graphene is particularly attractive as a platform for studying noncovalent molecular physisorption. Its perfect lattice ensures physisorption nature for molecular adsorption, and its linear band dispersion also enables a continuous gate tuning of the Fermi energy level.

The electrochemical response of nanomaterials has already been explored for a wide variety of applications like molecular recognition and separation[16−24] and even nanobiomimetics.[25−27] Despite these progresses, there still is a lack of understanding of the fundamental interactions between molecules and nanomaterials. For example, the chemical

Received: November 4, 2015
Revised: December 27, 2015
Published: December 28, 2015

DOI: 10.1021/acs.nanolett.5b04500
Nano Lett. 2016, 16, 695−700

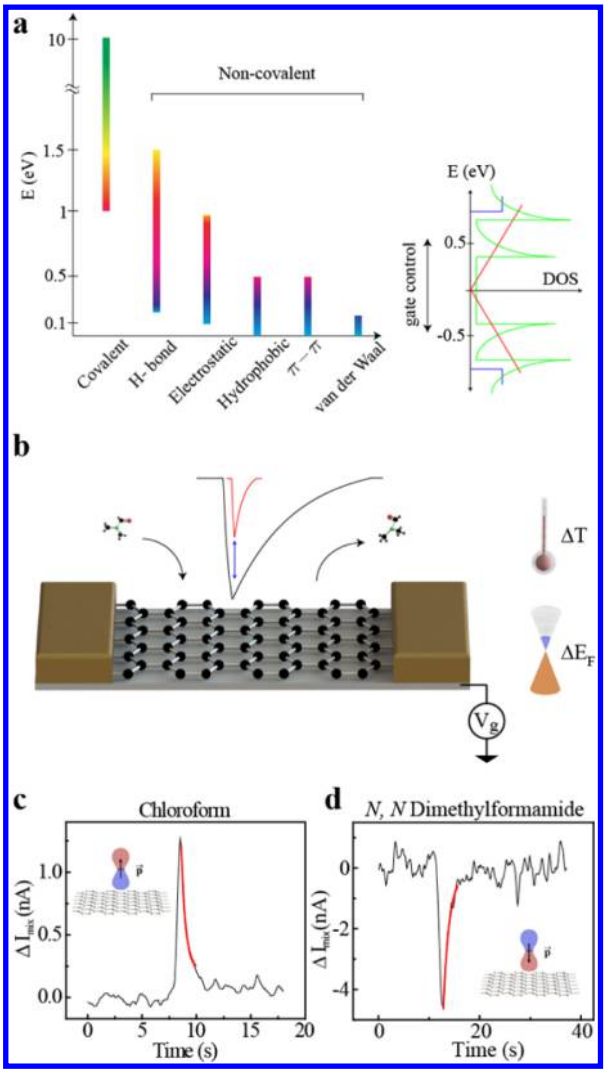

Figure 1. Electrical detection of molecular physisorption on graphene. (a) Representation of the energy scales for covalent and noncovalent molecular interactions. On the right is plotted the density of states for common one-dimensional (carbon nanotube in green) and two-dimensional (graphene in red and MoS2 in blue) materials with energy. Through an electrostatic gate one can shift graphene's Fermi level about ±0.5 eV in practical devices. (b) Schematic showing the physisorption and desorption of DMF molecule on graphene detected by graphene nanoelectronic heterodyne detector (black curve). Thermal or electrostatic activation can be used to tune the adsorption−desorption kinetics (from black to red curve). (c,d) Heterodyne mixing response of graphene to chloroform and DMF, respectively. The responses are reversible with instantaneous rise followed by an exponential decay. Exponential fits to decay curves are shown in red. The injected masses for chloroform and DMF are 2.85 and 4.72 ng, respectively. The back gate voltage (V_g) is 0 V and temperature (T) is 296.2 K. Insets show the orientation of respective molecule's dipole orientation on top of graphene.

response of most conventional nanoelectronic systems is driven by charge transfer via covalent binding with dangling bonds or defect sites,[16,17,28−31] which unfortunately does not represent the interaction between a charge neutral molecule and the perfect graphene lattice.[20,28,32] In this work, we instead analyze the noncovalent physisorption of polar molecules including chloroform, dichloromethane, chlorobenzene, 1,2-dichlorobenzene, dimethylmethylphosphonate (DMMP), and *N*,*N*- dimethylformamide (DMF) on graphene using a graphene nanoelectronic heterodyne sensor.[18,20] We demonstrate electrical probing of molecular physisorption on graphene by monitoring the interaction kinetics in real-time, and experimentally quantify the molecule-graphene binding affinities. Furthermore, we demonstrate for the first time electrical tuning of molecular physisorption through electrostatic gating of graphene.

We chose a graphene nanoelectronic heterodyne sensor[20] as our testbed to investigate molecular physisorption on the graphene surface. Briefly, graphene field effect transistors were integrated with a gas chromatography (GC) system[20] in order to generate a subsecond wide vapor pulse for real-time dynamic study of molecule−graphene interaction (see Supporting Information). A high frequency alternating current (ac) voltage was used to drive the adsorbed molecules' dipoles, which induces charge density fluctuations inside graphene. These charge density fluctuations are frequency-mixed with the ac excitation to generate a heterodyne mixing signal (see Supporting Information). In particular, the high-speed, high-sensitivity nature of the graphene heterodyne sensor[20] enables real-time monitoring of the molecular physisorption and desorption (Figure 1b, black curve). Furthermore, the interaction kinetics can be altered (Figure 1b, red curve) by changing the temperature or, more interestingly, by changing the chemical potential in graphene through electrostatic gating and recorded using the same sensor.

To prove the concept, we measured the time domain mixing current signal change upon adsorption and desorption of chloroform and DMF (Figure 1c,d, respectively). Reversible mixing current signal changes were observed with an instantaneous current jump followed by a slower decay. These events correspond to molecular adsorption and desorption on the graphene surface. In all the experiments carried out in this work, we consistently observed desorption to be dominated by a single exponential decay. Following first order rate kinetics, $R_{des} = Ae^{-k_{des}t}$, the desorption curve can be fit with an exponential to obtain the desorption rate, k_{des}, or desorption time, τ_{des} (= $1/k_{des}$). We obtained k_{des} of 2.5 and 0.82 s^{-1} and τ_{des} of 0.4 and 1.22 s for chloroform and DMF, respectively. We also note the opposite mixing current signal changes for the adsorption of chloroform and DMF, which is related to the orientation of their molecular dipoles with respect to the graphene plane; the electronegative (positive) side of chloroform (DMF) being closer to graphene results in a positive (negative) response, as explained in detail in our previous work.[20]

We further characterized the molecular binding affinities through temperature dependent measurements. In the absence of charge transfer, the weak interactive forces determine the ability of a molecule to adsorb onto graphene surface. The competing electronic repulsive forces and attractive van der Waals forces lead to the formation of a potential energy well, the minima of which determines the binding energy of molecule to graphene.[1] From the transition state theory,[4] molecular desorption process is governed by the binding energy, E_a, and the desorption rate, k_{des}, is given by

$$k_{des} = \nu_f e^{-(E_a/k_B T)} \quad (1)$$

where ν_f is the attempt frequency, k_B is the Boltzmann constant, and T is the temperature. Hence, measuring the temperature-dependent molecular desorption rates can yield the corresponding binding affinity.

DOI: 10.1021/acs.nanolett.5b04500
Nano Lett. 2016, 16, 695−700

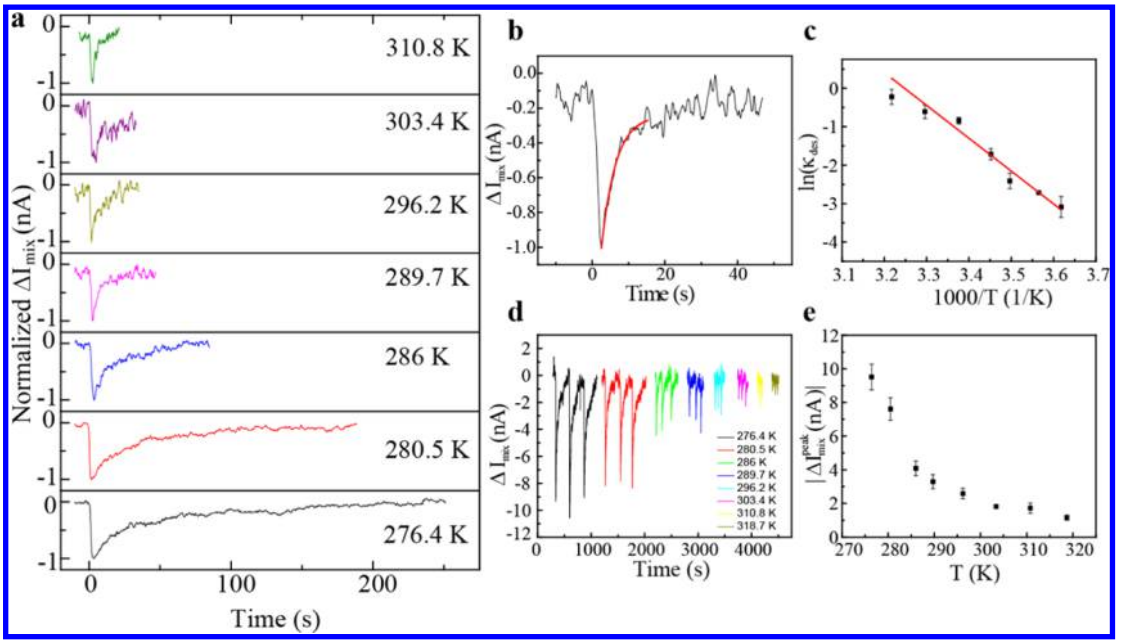

Figure 2. Electrical detection of temperature-dependent DMMP interaction with graphene. (a) Normalized graphene sensor's temporal response to 1.145 ng DMMP at different temperatures. (b) Graphene sensor's temporal response to DMMP at 289.7 K. Exponential fit (in red) to desorption curve yields desorption rate $k_{des} = 0.25\ s^{-1}$ ($\tau_{des} = 4$ s). (c) Desorption rates, k_{des}, plotted against temperature on the Arrhenius scale ($\ln k_{des} - 1/T$). Slope of the Arrhenius plot (linear fit in red) gives noncovalent binding energy $E_a = 734 \pm 52$ meV. (d) Temporal response to repeated doses of 1.145 ng of DMMP at different temperatures. (e) Temperature dependence of peak mixing current responses in (d). These measurements were done on graphene transistor with $L = 1\ \mu$m, $W = 1\ \mu$m, and back gate voltage was held at $V_g = 0$ V. Error bars in (c,e) show the standard deviation over 3 runs. All measurements were carried out in air and at atmospheric pressure.

Figure 2a shows the normalized time domain desorption curves for DMMP at different substrate temperatures. It is clear that the desorption rate is faster at higher temperatures. Similar to Figure 1c,d, the desorption rate at different temperatures can be extracted through an exponential fit, as shown in Figure 2b. Importantly, temperature-dependent physisorption responses provide a means to investigate interaction kinetics and determine corresponding binding energies.[4] Figure 2c shows an Arrhenius plot of temperature dependent desorption rates, k_{des}, obtained by exponential fits to the response curves at different temperatures shown in Figure 2d. The slope of the $\ln(k_{des}) - 1/T$ plot gives the molecule−graphene binding energy, which for DMMP is measured to be 734 ± 52 meV. Similar temperature dependent desorption rate studies for chloroform, dichloromethane, and DMF yield binding energies of 223 ± 13, 195 ± 10, and 657 ± 23 meV, respectively (see Supporting Information Figure S1).

We also studied the temperature dependence of peak mixing current intensity as shown in Figure 2e. The peak mixing currents at different temperatures were obtained from Figure 2d. It is clear that the peak mixing current decreases with increasing temperatures. This observation corroborates with the faster desorption rate at higher temperature, which reduces surface molecule concentration and hence the response signal. Above 310.8 K substrate temperature, the signal response for DMMP injection was within the noise floor.

In addition to temperature, the back gate electrode can provide another knob to tune the Fermi level of graphene, and hence control the behavior of molecular species on top of graphene.[33] To prove the concept, we studied the gate tuning of molecular desorption on graphene. Figure 3a shows desorption curves of chloroform at several different gate voltages. Importantly, the molecular desorption rates can be drastically altered through electrostatic gating without the need of changing substrate temperature. We further extract the chloroform desorption rates, k_{des} ($1/\tau_{des}$), and plot them against the gate voltage and Fermi level shifting from Dirac point of graphene in Figure 3b. It is clear that more positive gate voltages and higher Fermi levels weaken chloroform physisorption on graphene, leading to a higher desorption rate. Moreover, the reduced mixing current peak intensity at more positive gate voltages (Figure 3c) also confirms the weakening of chloroform physisorption. Significantly, this is the first time that electrical tuning of molecular physisorption has been demonstrated.

We further investigated the gate-controlled molecular physisorption of DMF, which has opposite dipole orientation compared to chloroform. Active gate tuning of molecular desorption rate was observed once again (Figure 3d). Interestingly, contrary to chloroform, more positive gate voltages and higher Fermi levels strengthen DMF physisorption on graphene, leading to slower desorption rate (Figure 3e). This is further corroborated by the enhanced mixing current peak intensity at more positive gate voltages (Figure 3f). The opposite trend for the gate tuning of chloroform and DMF desorption can be attributed to their opposite dipole orientations on top of graphene.[20] The gate-induced electrostatic doping in graphene shifts graphene's chemical potential, leading to changes of the molecular binding affinity on graphene. For chloroform physisorption, the electronegative side of its dipole sits closer to graphene.[20] A positive gate voltage raises the chemical potential of graphene, thus decreasing the binding affinity between graphene and chloroform. On the other hand, DMF has the electropositive side of its dipole located above graphene. A positive gate voltage leads

DOI: 10.1021/acs.nanolett.5b04500
Nano Lett. 2016, 16, 695−700

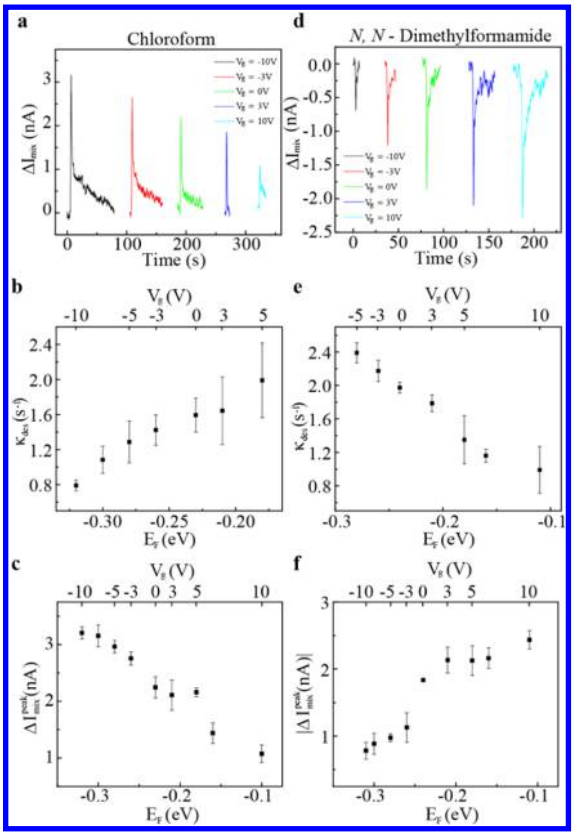

Figure 3. Electrical tuning of molecular physisorption on graphene. (a,d) Graphene mixing current response for chloroform and DMF at different back-gate voltages, respectively. (b,e) Desorption rates, k_{des}, obtained from the exponential fits to the mixing current responses to repeated doses of chloroform and DMF, respectively, plotted against graphene Fermi level shift and the applied gate voltage. (c,f) Peak mixing current response of chloroform and DMF respectively, plotted against Fermi level shift and the applied back-gate voltage. The measurements were carried out on two different devices with same dimensions, L = 1 μm and W = 2 μm. The injected masses for chloroform and DMF were 285 and 18.88 ng, respectively. Error bars in (c−f) show the standard deviation over three runs. All measurements were carried out in air at atmospheric pressure and room temperature (296.2 K).

to higher graphene chemical potential and increases the binding affinity between graphene and DMF.

Noncovalent modification of graphene lattice with aromatic chemical compounds is widely pursued to enhance or tailor the electronic and optical properties of graphene.[34] The planar sp^2-hybridized graphene lattice also makes it a perfect substrate to study $\pi-\pi$ interactions, which has been a topic of intense research, albeit mostly theoretical and controversial.[35−38] Here, we chose chlorobenzenes as model systems to study arene−graphene interaction. Chlorobenzenes are important chemicals for industry since they are widely used in deodorants, insect repellents, and pesticides synthesis processes, and they are also notorious for being environmental pollutants.[39] Figure 4a shows the normalized adsorption/desorption curves of 1,2-dichlorobenzene (DCB) on graphene at different substrate temperatures. The most favored orientation of DCB on graphene[40] is offset parallel stacking[36,38] where local polar C−Cl bonds lie directly atop the graphene π-electron cloud (Figure 4b). Using first order rate kinetics, desorption rate (k_{des}) for DCB at each temperature (Supporting Information Figure S2) is extracted and the corresponding Arrhenius plot is shown in Figure 4c. The slope of the $\ln(k_{des}) - 1/T$ gives DCB-graphene binding energy of 447 ± 24 meV. The temperature-dependence desorption trend for DCB agrees with the other nonaromatic molecules reported in this study, and the temperature-dependent peak mixing currents (Figure 4d) also confirms faster desorption with increasing temperatures. Interestingly, the peak mixing current response to DCB was found to saturate at lower temperatures as shown in Figure 4a,d. We observed the same effect with chlorobenzene where peak current saturation occurred at temperature below 289.7 K as well (see Supporting Information Figure S1). The current saturation may be due to surface saturation with a layer of DCB, which screens the electric field for additional layer of DCB on graphene. Further in-depth studies are needed in order to fully understand this interesting phenomenon.

We also studied the effect of gate induced Fermi level tuning on DCB adsorption on graphene. Figure 4e shows graphene response to DCB at different gate voltages. Interestingly, the extracted desorption rates, k_{des}, show little gate dependence (Figure 4f), and the peak mixing current increases only slightly even with a ΔE_F shift of ∼200 meV (Figure 4g). Careful transport studies on DCB-decorated graphene transistor suggest that the electric field screening from DCB molecules is not the reason for the weak gate tuning of DCB desorption dynamics (see Supporting Information Figure S6 and Discussion). Another possible explanation may be that in an offset parallel stacked structure as the electron density of graphene increases, the dispersive interaction between local polar C−Cl bonds and graphene π-electrons counters the offset $\pi-\pi$ repulsion between the two systems.[38] Similar gate dependence is observed for chlorobenzene as well (Supporting Information Figure S3). The temperature- and electric field-dependent behavior of aromatic compounds shed new light into the complex $\pi-\pi$ stacked systems, a detailed understanding of which can play a key role in a wide range of applications like drug discovery, protein-nucleic acid recognition, proteomics, and crystal packing.

Finally, we summarize the experimentally obtained binding energies and attempt frequencies of various molecules on graphene in Table 1 along with their dipole moments and polarizability values. The mixing current response relates to the molecular adsorbates' dipole moment,[20] but it is not surprising that the binding energies do not exactly follow the dipole moment strength of molecules. The mixing current response is a direct manifestation of physisorption of molecules, where weak van der Waals forces include contributions from both permanent and induced dipoles, and therefore the binding energy is affected by both dipole moment and the polarizability of the molecules.[1] We note that the graphene devices typically have intrinsic environmental doping that can shift the Fermi levels away from the Dirac point even without gating. This intrinsic Fermi level shift can affect the molecular binding affinity in the same way as electrostatic gating. Hence, we list the intrinsic Fermi level offsets for graphene devices used in the last column of Table 1.

Until now, the study of noncovalent molecule−nanomaterial interactions have been confined mostly to the theoretical realm. Our results provide an experimental benchmark for future investigation of such fundamental processes, especially in graphitic systems. Furthermore, the gate controlled tuning of adsorbate−graphene interactions provides new opportunities to implement precise on-chip chemical control that can

DOI: 10.1021/acs.nanolett.5b04500
Nano Lett. 2016, 16, 695−700

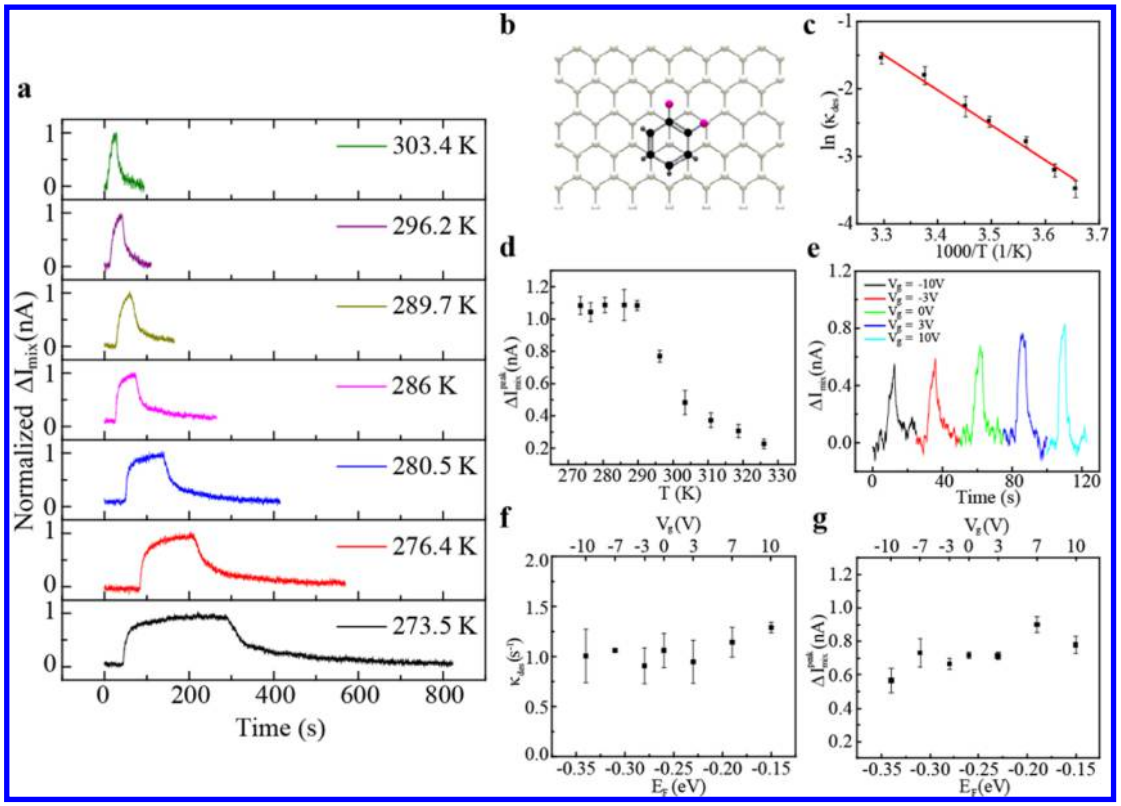

Figure 4. Electrical detection and tuning of noncovalent interactions between aromatic compounds and graphene. (a) Normalized graphene sensor's temporal responses to 130 ng DCB at different temperatures. (b) Schematic illustration of most favored offset-parallel stacked orientation of DCB on top of graphene. (c) Desorption rates, k_{des}, obtained by exponential fits to the temporal response to repeated doses of DCB at different temperatures, plotted against temperature on Arrhenius scale ($\ln k_{des} - 1/T$). Slope of Arrhenius plot (linear fit in red) gives noncovalent binding energy E_a = 447 ± 24 meV. (d) Temperature dependence of peak mixing current response to repeated doses of DCB. These measurements were done on graphene transistor with L = 5 μm, W = 1 μm, and back gate voltage was held at V_g = 0 V. Error bars in (c,d) show the standard deviation over three runs. All measurements were carried out in air and at atmospheric pressure. (e) Mixing current responses to DCB at different back-gate voltages. (f) Desorption rates, k_{des}, plotted against Fermi level shift and the applied back-gate voltage. (g) Peak mixing current response to repeated doses of DCB plotted against Fermi level shifts and the applied back-gate voltage. The measurements were carried out on a device with L = 1 μm and W = 2 μm. Error bars in (f,g) show the standard deviation over three runs. All measurements were carried out in air at atmospheric pressure and room temperature (296.2 K).

Table 1. Experimental Binding Energy (E_{bind}^{exp}, meV) and Attempt Frequency (ν_f, s^{-1}) for Polar Molecules on Graphene Tabulated along with Molecule's Dipole Moment (D, Debye), Polarizability (α, 10^{-24} cm^3), and Graphene's Fermi Level Offset from the Dirac Point (ΔE_F^0, meV, see Supporting Information)

	D	α	E_{bind}^{exp}	ν_f	ΔE_F^0
chloroform	1.04	8.23	223 ± 13	1.23×10^4	−160
dichloromethane	1.6	6.48	195 ± 10	3.71×10^3	−250
chlorobenzene	1.54	12.3	367 ± 30	1.79×10^6	−240
1,2 dichlorobenzene	2.5	14.17	447 ± 24	6.32×10^6	−250
DMMP	3.62	10	734 ± 52	1.10×10^{12}	−220
DMF	3.82	7.8	657 ± 23	3.57×10^{10}	−150

revolutionize areas of catalysis, drug design, biochemical recognition, and environmental remediation, just to name a few.

■ ASSOCIATED CONTENT

Supporting Information

The Supporting Information is available free of charge on the ACS Publications website at DOI: 10.1021/acs.nanolett.5b04500.

Sample fabrication and characterization, measurement setup, additional experimental data and figures. (PDF)

■ AUTHOR INFORMATION

Corresponding Authors

*E-mail: xsfan@umich.edu.

*E-mail: zzhong@umich.edu.

Present Address

(K.R.) KLA Tencor, Milpitas, California 95035, U.S.A.

Notes

The authors declare no competing financial interest.

■ ACKNOWLEDGMENTS

This work was supported by the National Science Foundation under ECCS-1405870, DMR-1120187, and IIP-1443335 grants. Devices were fabricated in the Lurie Nanofabrication Facility at University of Michigan, a member of the NSF National Nanotechnology Infrastructure Network.

■ REFERENCES

(1) Israelachvili, J. *Intermolecular and Surface Forces*, 3rd ed.; Academic Press: Waltham, MA, 2011.

(2) Frieden, E. *J. Chem. Educ.* **1975**, *52* (12), 754−761.

DOI: 10.1021/acs.nanolett.5b04500
Nano Lett. 2016, 16, 695−700

(3) Hobza, P.; Müller-Dethlefs, K. *Non-covalent Interactions: Theory and Experiment*; The Royal Society of Chemistry: Cambridge, UK, 2010.
(4) Somorjai, G. A. *Introduction to Surface Chemistry and Catalysis*; John Wiley and Sons: New York, 1994.
(5) Strmcnik, D.; Kodama, K.; van der Vliet, D.; Greeley, J.; Stamenkovic, V. R.; Markovic, N. M. *Nat. Chem.* **2009**, *1* (6), 466−472.
(6) Berezhkovskiy, L. M. *Expert Opin. Drug Metab. Toxicol.* **2008**, *4* (12), 1479−1498.
(7) Goyal, M.; Rizzo, M.; Schumacher, F.; Wong, C. F. *J. Med. Chem.* **2009**, *52* (18), 5582−5585.
(8) Burley, S. K.; Petsko, G. A. *Adv. Protein Chem.* **1988**, *39*, 125−189.
(9) Ramstrom, O.; Lehn, J. M. *Nat. Rev. Drug Discovery* **2002**, *1* (1), 26−36.
(10) Lehn, J. M. *Angew. Chem., Int. Ed. Engl.* **1990**, *29* (11), 1304−1319.
(11) Mauter, M. S.; Elimelech, M. *Environ. Sci. Technol.* **2008**, *42* (16), 5843−5859.
(12) Lu, W.; Lieber, C. M. *Nat. Mater.* **2007**, *6*, 841−850.
(13) Geim, A. K.; Novoselov, K. S. *Nat. Mater.* **2007**, *6*, 183−191.
(14) McEuen, P. L. *Phys. World* **2000**, *13*, 31−36.
(15) Wang, Q. H.; Kalantar-Zadeh, K.; Kis, A.; Coleman, J. N.; Strano, M. S. *Nat. Nanotechnol.* **2012**, *7*, 699−712.
(16) Zheng, G. F.; Patolsky, F.; Cui, Y.; Wang, W. U.; Lieber, C. M. *Nat. Biotechnol.* **2005**, *23*, 1294−1301.
(17) Kong, J.; Franklin, N. R.; Zhou, C.; Chapline, M. G.; Peng, S.; Cho, K.; Dai, H. *Science* **2000**, *287*, 622−625.
(18) Kulkarni, G. S.; Zhong, Z. *Nano Lett.* **2012**, *12*, 719−723.
(19) Duan, X.; Li, Y.; Rajan, N. K.; Routenberg, D. A.; Modis, Y.; Reed, M. A. *Nat. Nanotechnol.* **2012**, *7* (6), 401−407.
(20) Kulkarni, G. S.; Reddy, K.; Zhong, Z.; Fan, X. *Nat. Commun.* **2014**, *5*, 4376.
(21) Yang, R.; Tang, Z.; Yan, J.; Kang, H.; Kim, Y.; Zhu, Z.; Tan, W. *Anal. Chem.* **2008**, *80* (19), 7408−7413.
(22) Liu, G.; Rumyantsev, S. L.; Jiang, C.; Shur, M. S.; Balandin, A. A. *IEEE Electron Device Lett.* **2015**, *36* (11), 1202−1204.
(23) Rumyantsev, S.; Liu, G.; Shur, M. S.; Potyrailo, R. A.; Balandin, A. A. *Nano Lett.* **2012**, *12* (5), 2294−2298.
(24) Samnakay, R.; Jiang, C.; Rumyantsev, S. L.; Shur, M. S.; Balandin, A. A. *Appl. Phys. Lett.* **2015**, *106* (2), 023115.
(25) Potyrailo, R. A.; Ghiradella, H.; Vertiatchikh, A.; Dovidenko, K.; Cournoyer, J. R.; Olson, E. *Nat. Photonics* **2007**, *1* (2), 123−128.
(26) Garcia-Fandino, R.; Sansom, M. S. P. *Proc. Natl. Acad. Sci. U. S. A.* **2012**, *109* (18), 6939−6944.
(27) Dang, X.; Yi, H.; Ham, M.-H.; Qi, J.; Yun, D. S.; Ladewski, R.; Strano, M. S.; Hammond, P. T.; Belcher, A. M. *Nat. Nanotechnol.* **2011**, *6* (6), 377−384.
(28) Kumar, B.; Min, K.; Bashirzadeh, M.; Farimani, A. B.; Bae, M. H.; Estrada, D.; Kim, Y. D.; Yasaei, P.; Park, Y. D.; Pop, E.; Aluru, N. R.; Salehi-Khojin, A. *Nano Lett.* **2013**, *13* (5), 1962−1968.
(29) Salehi-Khojin, A.; Lin, K. Y.; Field, C. R.; Masel, R. I. *Science* **2010**, *329*, 1327−1330.
(30) Lee, C. Y.; Strano, M. S. *Langmuir* **2005**, *21*, 5192−5196.
(31) Lazar, P.; Karlicky, F.; Jurecka, P.; Kocman, M.; Otyepkova, E.; Safarova, K.; Otyepka, M. *J. Am. Chem. Soc.* **2013**, *135* (16), 6372−6377.
(32) Dan, Y.; Lu, Y.; Kybert, N. J.; Luo, Z.; Johnson, A. T. C. *Nano Lett.* **2009**, *9*, 1472−1475.
(33) Riss, A.; Wickenburg, S.; Tan, L. Z.; Tsai, H.-Z.; Kim, Y.; Lu, J.; Bradley, A. J.; Ugeda, M. M.; Meaker, K. L.; Watanabe, K.; Taniguchi, T.; Zettl, A.; Fischer, F. R.; Louie, S. G.; Crommie, M. F. *ACS Nano* **2014**, *8* (6), 5395−5401.
(34) Georgakilas, V.; Otyepka, M.; Bourlinos, A. B.; Chandra, V.; Kim, N.; Kemp, K. C.; Hobza, P.; Zboril, R.; Kim, K. S. *Chem. Rev.* **2012**, *112* (11), 6156−6214.
(35) Zhou, P.-P.; Zhang, R.-Q. *Phys. Chem. Chem. Phys.* **2015**, *17* (18), 12185−12193.
(36) Hunter, C. A.; Sanders, J. K. M. *J. Am. Chem. Soc.* **1990**, *112* (14), 5525−5534.
(37) Cozzi, F.; Cinquini, M.; Annuziata, R.; Siegel, J. S. *J. Am. Chem. Soc.* **1993**, *115* (12), 5330−5331.
(38) Wheeler, S. E. *J. Am. Chem. Soc.* **2011**, *133* (26), 10262−10274.
(39) Hill, G. A.; Tomusiak, M. E.; Quail, B.; Vancleave, K. M. *Environ. Prog.* **1991**, *10* (2), 147−153.
(40) Zhang, Y.-H.; Zhou, K.-G.; Xie, K.-F.; Zhang, H.-L.; Peng, Y.; Wang, C.-W. *Phys. Chem. Chem. Phys.* **2012**, *14* (33), 11626−11632.

DOI: 10.1021/acs.nanolett.5b04500
Nano Lett. 2016, 16, 695−700